Presented at the 1997 IEEE Nuclear Science Symposium,
Albuquerque, New Mexico, November 9-15, 1997

BNL 64949

Published as:
IEEE Transactions on Nuclear Science, NS-45 (1998) 1024-1033

A Portable Gamma-Ray Spectrometer Using Compressed Xenon*

G. J. Mahler, B. Yu, G. C. Smith, W. R. Kane and J. R. Lemley

Brookhaven National Laboratory

Upton, NY 11973-5000

November 1997

*** This research was supported by the US Department of Energy under Contract No. DE-AC02-76CH00016.**

A Portable Gamma-Ray Spectrometer Using Compressed Xenon*

G. J. Mahler, B. Yu, G. C. Smith, W. R. Kane and J. R. Lemley
Brookhaven National Laboratory, Upton, NY 11973-5000

Abstract

An ionization chamber using compressed xenon has been designed and built for gamma-ray spectrometry. The device is based on signal measurement from a parallel plate detector, with the gas enclosure constructed specifically for packaging into a portable instrument; thus, appropriate engineering practices using ASME codes have been followed. The portable system comprises two small containers that can be setup for operation in just a few minutes. Its sensitivity is 100 keV to over 1 MeV, with a resolution at 662 keV of 2.5% FWHM for uniform irradiation, and 2% FWHM for collimated irradiation, comparable to the best ever with compressed xenon. It also exhibits greater specificity than most scintillators, such as NaI. The device is insensitive to neutron damage and has a low power requirement.

I. INTRODUCTION

There is an important requirement in the areas of environmental monitoring, nuclear safeguards and geophysics for low power, high-resolution gamma-ray spectrometers that are portable and capable of remote operation. Germanium and NaI detectors are now commonly used. In certain circumstances, the above conditions may be fulfilled more appropriately by two other, promising, techniques. These are detectors based on xenon gas, and detectors based on CdZnTe. We present here a description of a portable, compressed xenon spectrometer that is, we believe, one of a few developments of this technology to progress from the bench-top to field use capability.

II. BACKGROUND

The variance of *N*, the number of electron-ion pairs generated in a detector medium by an incoming photon, is given by:

$$\sigma_N^2 = FN. \quad (1)$$

The Fano factor, *F*, [1] accounts for the fluctuations in *N* being smaller than (random) Poissonian statistics. Taking as an example the 662 keV gamma-ray line from Cs^{137}, eq. (1) predicts an energy resolution of 0.56% FWHM in xenon (assuming the energy required to generate one electron-ion-pair, and *F*, are 21.9 eV and 0.17 respectively [2]). This excellent intrinsic resolution, combined with a high atomic number, shows xenon is an attractive medium for high-resolution gamma-ray detection. Xenon exhibits a highly nonlinear behavior of density against pressure, and is very compressible near its critical point, which corresponds to 58 bar, ρ = 1.1 g/cm^3 and 17ºC [3]. Some thermodynamic properties of xenon are shown in figure 1 in the form of isotherms [4]. These illustrate the remarkable property of xenon, that very little increase in pressure occurs, at room temperature, for significant increases in density. Nevertheless, when engineering a pressure vessel for field operation, due account must be taken of the large increase in pressure that occurs with increasing temperature, at a given density.

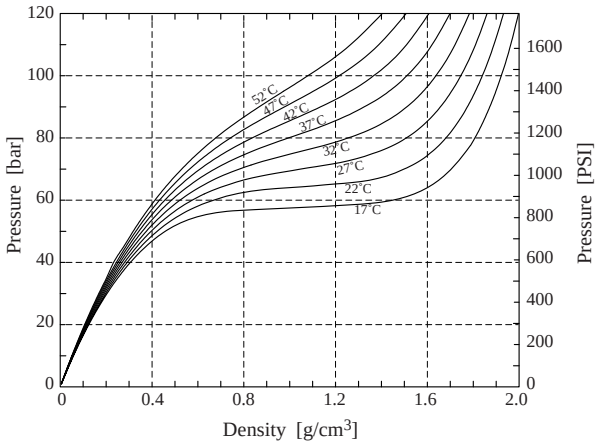

Figure 1. Isotherms of xenon. The detector vessel used in the portable system contained xenon with ρ = 0.55 g/cm^3.

The design of an ionization chamber suitable for spectrometry with xenon is most conveniently based on electrodes with cylindrical geometry [5] or electrodes with parallel plate geometry [6,7,8]. In this initial work we have chosen a parallel plate design because a linear drift field was necessary for determining some basic characteristics of the system. The fundamental design principles of the device are quite simple, with the important components shown schematically in figure 2. The sensitive volume is defined by a cathode, two drift-field defining electrodes, and an anode. Absorption of a photon in the active volume creates electron-ion pairs; the electrons then drift to the anode. In order to prevent pulse amplitude dependence on conversion depth, and to decrease the electron signal risetime, a Frisch grid [9] is placed close to the anode. The elec-

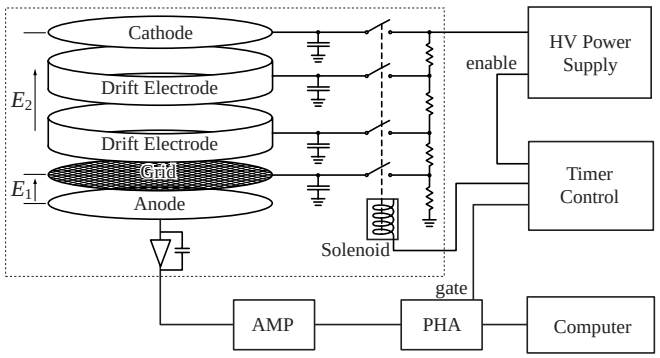

Figure 2. Schematic of major components. For portable system, components within dashed rectangle are in aluminum container, the remainder are in second container (see fig.8).

* This research was supported by the US Department of Energy: Contract No. DE-AC02-76CH00016.

tron signal induced on the anode is collected by a low-noise charge sensitive preamplifier and shaping amplifier; a pulse height analyzer records the spectrum.

Electron transport in compressed xenon is extremely sensitive to impurity. Typical requirements are that electronegative impurities be maintained below 0.5 ppm. In general, previous workers have identified two levels of performance. The first level is that which can be attained by using a high-temperature getter and appears to permit good performance up to densities of about 0.6 g/cm^3. Beyond this density other techniques based on titanium spark discharge have been employed to lower impurity levels further, which in turn maintains good performance. A crucial element in the detector design is that absolutely no organic materials can be used; outgassing of electronegative vapors even on a small scale will degrade the operation of the detector.

III. Apparatus

A. Detector

The detector components in figure 2 have been engineered into a pressure vessel made from a high-strength titanium-aluminum-vanadium alloy (Ti-6Al-4V). All internal electrodes have been fabricated from either stainless steel, nickel and aluminum, and insulators from macor ceramic. The electrode arrangement is shown in figure 3. The base is a 17 cm diameter flange, 2.9 cm thick, with five 20kV HT feed-throughs installed in position using vacuum-brazing technology [10]. The five main electrodes are each held at five attachment points on ceramic pillars that are mounted to the baseplate with stainless steel supports. Notches in the ceramic pillars, together with wavy washers and split rings, ensure the electrodes are rigidly held in position. The anode and cathode are stainless steel plates, while the drift defining electrodes are stainless steel annuli. The grid consists of electroformed nickel mesh, 1.4 mm pitch, 90 μm wire width and 25 μm thickness, sandwiched between ceramic and aluminum annuli. An important requirement of the grid is a high level of tautness, which is necessary to minimize microphonic signals. The 6.4 cm open diameter of the grid defines the usable area of the device. Cathode-grid separation is 5.3 cm, and grid-anode separation is 0.7 cm. The five electrodes are electrically connected to their respective feed-throughs by stainless steel wire. We define E_1 as the field between anode and grid, and E_2 as the (drift) field between grid and cathode.

The assembly in figure 3, with a cover installed, completes the detector (pressure) vessel, which is shown in figure 4. The entrance window, facing down, is 7.6 cm in diameter and 6.35 mm thick, allowing good gamma transmission above 100 keV. Bolted to the outside of the titanium flange with a mini-conflat flange is a short length of stainless steel pipe, containing a pressure transducer [11], rupture disk and all-metal valve. The mini-conflat flange at the other end permits attachment of the detector to the gas-filling system.

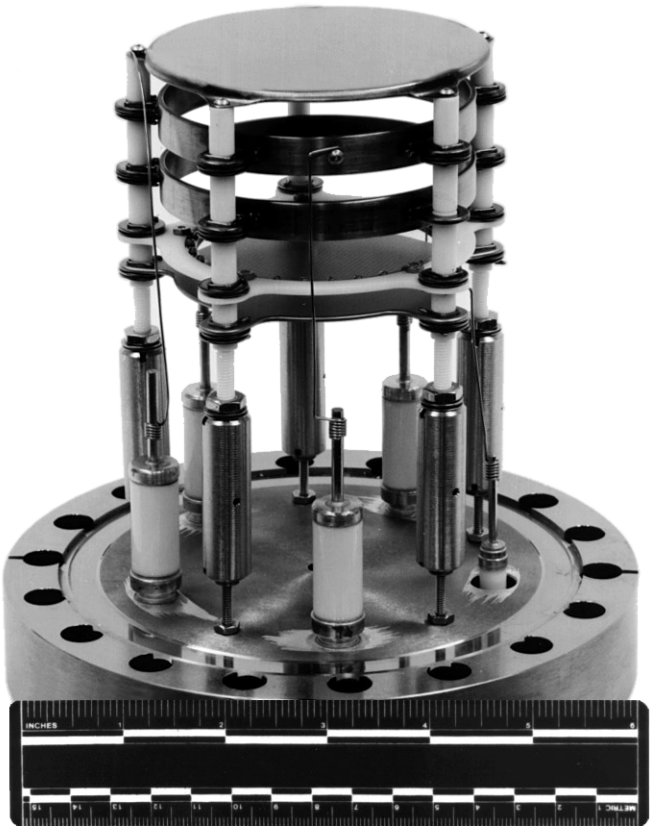

Figure 3. Photograph of internal components of detector vessel, before cover is in place. Cathode, drift electrodes, grid and anode are supported by ceramic pillars, in top half of picture.

Figure 4. Photograph of complete detector (pressure) vessel, with cover bolted to flange (inverted compared to fig. 3).

B. Gas-filling system

A gas purification and filling system, based on high-temperature getters [12] has been designed and fabricated, and is shown schematically in figure 5. It is constructed from ½ inch OD stainless steel pipe using orbital welding techniques whenever possible; a small number of mini-conflat flanges with copper gaskets are used and valves are of all-metal construction. Evacuation is accomplished with a molecular drag pump, followed by a 60 liter/s Starcell ion pump.

IV. Preparation and Filling

The gas-filling system, with detector vessel attached, is baked out and pumped for several days. Research grade purity xenon is then transferred from the commercial cylinder to storage cylinder B. This is carried out by cooling the latter to liquid nitrogen temperature, where the SVP of xenon is a fraction of a torr. The gas can then be further purified by transferring the xenon backwards and forwards, using the same cryogenic technique, between storage cylinders A_1 /A_2 and B; each time the gas makes one pass through the high temperature getters. Gas is finally admitted to the detector by cooling its cover only to about -74ºC, with dry ice and alcohol, which limits thermal stress to the detector components compared with liquid nitrogen temperature.

This procedure requires the utmost performance from the seal between the titanium flange and cover; it must be bakeable and leak-tight both for UHV and for pressures approaching 60 bar and above. We have tried several commercially available metal seals; the most reliable operation has been obtained using a spring-energized metal C-ring [13].

Measurement of the correct density of xenon is a difficult task, even with a pressure transducer directly on the detector housing. The isotherms in figure 1 show that, at a given density, there is a significant temperature dependence on pressure, which becomes particularly significant above 0.4 g/cm^3. Furthermore, the high compressibility of xenon above 0.4 g/cm^3 results in density being relatively insensitive to pressure up to densities of 1.5 g/cm^3. These characteristics require that temperature and, particularly, pressure are measured with extreme accuracy. Instead, we measured the mass of the detector vessel at vacuum, and again with the final xenon filling. This represented a mass difference of about 1 kg. Mass and volume, and therefore density, can be determined to at least one percent. A technique has recently been described [14] in which the dependence of dielectric constant on density is used, a potentially more convenient method.

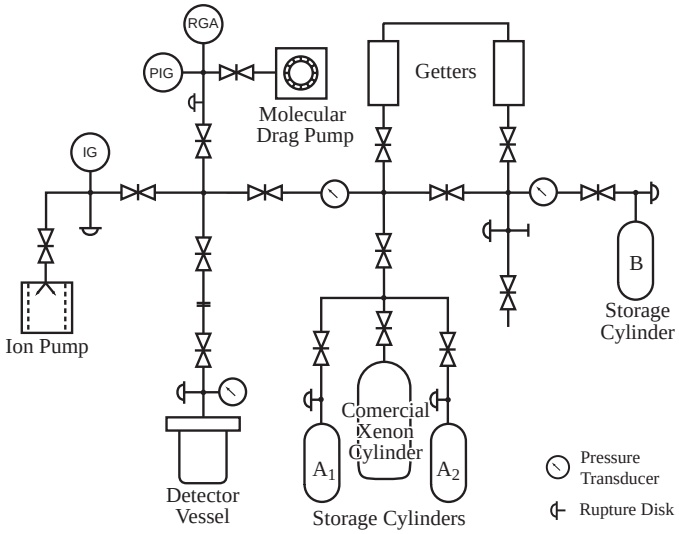

Figure 5. Gas purification and filling system.

In general about ten successive passes through the high temperature getter were necessary to obtain the required purity; preliminary measurements were carried out with the detector before packaging it into a portable system. Electron drift velocity has been determined as follows. The back-to-back 511 keV gamma-rays from a Na^{22} source were collimated with one beam directed through the side wall into the detector vessel perpendicular to the drift field, and the opposite beam onto a NaI scintillator detector. The gamma absorbed by the scintillator produces a prompt start signal, and the gamma absorbed in the detector produces electrons that drift and reach the anode to provide a stop signal. By probing different regions along the drift field, these timing measurements yield drift velocity, shown in figure 6.

Electron lifetime has been determined with the aforementioned experimental arrangement; Cs^{137} has also been used for this particular determination. The fraction of electrons surviving after drifting a time, t, with a lifetime τ, is given by

$$f_a = e^{-t/\tau} \quad . \qquad (2)$$

f_a can be determined by measuring the relative drop in anode pulse height as a function of position along the drift region at which the beam converts in the detector, and t is determined from drift velocity. Hence τ can be evaluated using eq.(2).

Measurements at 0.55 g/cm^3, with E_2 = 2 kV/cm, yielded a lifetime of around 5 ms. Thus, the maximum drift time of electrons is about 1% of the electron lifetime, resulting in a maximum loss of 1% of electrons. Lifetime progressively decreases as E_2 decreases; such field dependent lifetime is in agreement with previous results [6,14]. Moreover, we have found that,

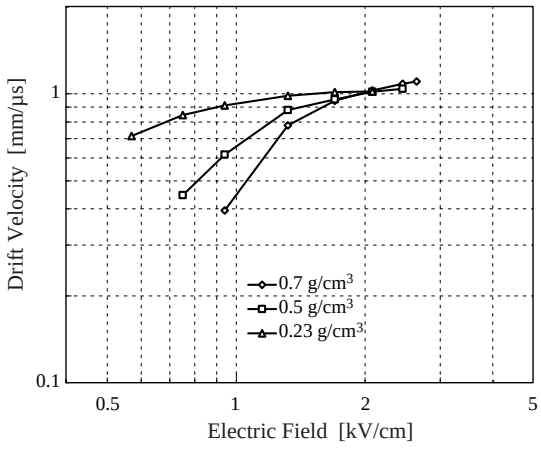

Figure 6. Measured electron drift velocity vs electric field.

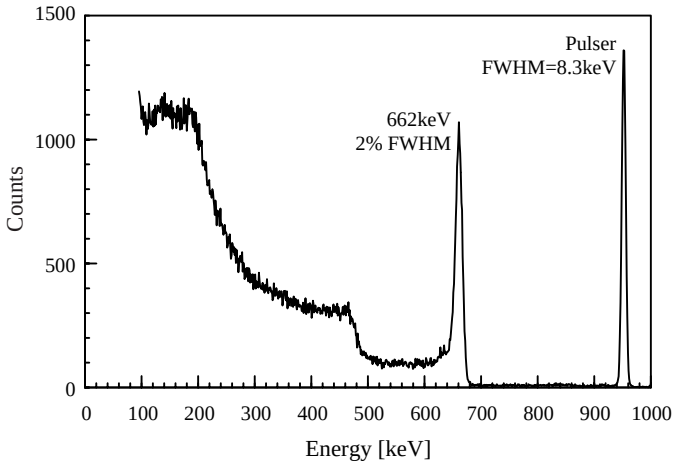

Figure 7. Anode pulse height spectrum of 662 keV gamma-rays from Cs^{137}. Collimated photons enter detector through side-wall, at right angles to drift field. Pulser response indicates electronic noise.

even with E_2 = 2 kV/cm, electron lifetime drops significantly below 1 ms for densities in excess of 0.6 g/cm^3. These observations are consistent with those of a recent detailed study [15], which found that the level of purification required for densities above about 0.6 g/cm^3 is difficult to achieve with high-temperature getters.

Figure 7 shows a Cs^{137} pulse height spectrum taken during the lifetime measurements. Since the collimated gamma-ray beam is perpendicular to the drift-field, broadening effects due to electron lifetime and grid shielding inefficiency are minimized. The FWHM of 2%, or 13.2 keV, is one of the best recorded in a compressed xenon detector. Also shown in the figure is the response to charge injection, from a pulser, of the electronics, which is seen to contribute just over 8 keV. This represents one of the main limitations of the detector performance, particularly at lower energies.

V. Portable System

With a xenon filling of 0.55 g/cm^3, the detector vessel has been incorporated into a portable system which contains the hardware and controls schematically illustrated in figure 2. A photograph of the portable system is shown in figure 8. The aluminum container on the left houses the detector, HT capacitors on the four non-ground electrodes, the high voltage relay, and the preamplifier. The second container on the right houses the high voltage supply, timer control, PHA, batteries, and has space for a laptop computer on which the analyzed spectrum is displayed. The preliminary measurements from section IV indicate that a drift-field, $E_2 \sim$ 2 kV/cm, is necessary for high resolution operation. A field ratio, $E_1/E_2 \geq 3$ allows nearly 100% transfer of electrons from the drift-region, through the grid, to the anode. These conditions are satisfied with −15 kV applied to the cathode (with anode at ground). Since we observed no evidence of corona, or other high voltage problems, up to ~ 19kV in the initial testing, 15 kV was deemed a comfortable voltage for field operation of the device. A resistive divider provides appropriate voltages to the drift electrodes and grid.

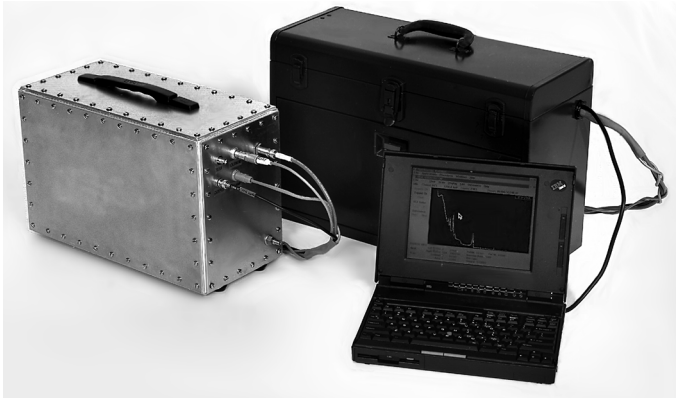

Figure 8. Photograph of portable system. Hermetically-sealed aluminum container, at left, houses detector vessel; detector window is at opposite end to cable connections. Contents of each container are shown in fig.2.

Even with good filtering, the high voltage supply contributes some broadening to gamma peaks because of ripple. This is completely overcome by charging the capacitors attached to the four non-ground electrodes and performing pulse height analysis when the supply is switched off. A timer control disables the PHA for the short charging time (approximately 10s), which is performed about every half-hour to prevent voltage droop. The duty cycle is thus very high, and this operational mode also reduces power consumption.

Figure 9 shows a spectrum from the portable system, under battery power, that combines the gamma-ray lines from Ba^{133}, Cs^{137} and Co^{60}. Irradiation was carried out from the front with no collimation. The FWHM of the Cs^{137} peak is about 2.5%; the extra broadening, compared with the side-collimated spectrum in figure 7, is due to the combined effects of electron lifetime and shielding inefficiency of the grid. It is believed that the Co^{60} peaks are broader than expected from a $1/E^{½}$ relationship because the range of the photoelectron is large enough to cause ballistic deficit effects due to the finite shaping time.

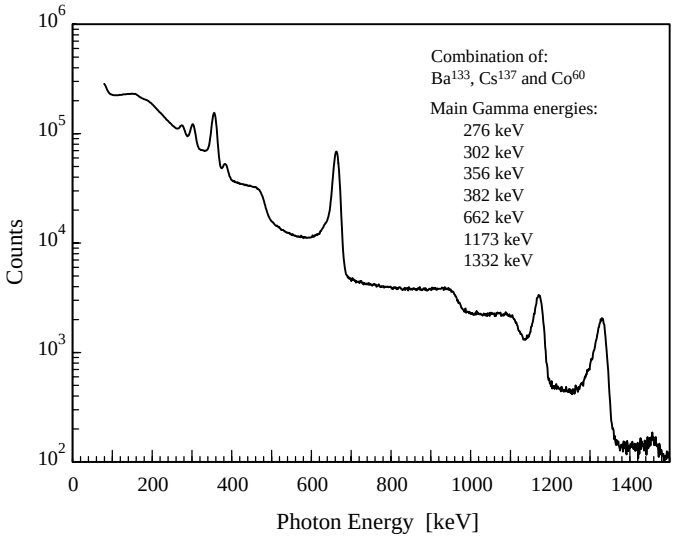

Figure 9. Performance of portable system under battery power. This shows pulse height spectrum for uniform irradiation through detector window, from Ba^{133}, Cs^{137} and Co^{60} sources.

Table 1.
Important Characteristics of Gamma-ray Spectrometer

Energy Range	100keV to ~1 MeV
Sensitive Volume	160 cm^3
Sensitive area	30 cm^2
Xenon density	0.55 g/cm^3
Drift Electric field	2 kV/cm
Maximum Electron Drift Time	~50 μs
Electron Lifetime	About 5ms @ 2kV/cm
Energy Resolution @ 662 keV	2.5 % FWHM
Efficiency @ 200keV/662 keV	40%/15% total, 30%/2% photoelectric
Detector Mass	10 kg
Portable System Mass	Two 20 kg containers
Power Consumption	7W (under development: ~ 1W)

VI. Conclusion

We have described the design and fabrication of a new, portable, low-power gamma-ray spectrometer; table 1 shows some important characteristics. The system can be powered into operation in just a couple of minutes, and will operate on batteries for several hours. The detection medium is based on compressed xenon, and it has been shown possible to engineer a pressure vessel according to ASME code suitable for practical use. The detector vessel has been in operation for over half a year, and has shown no signs of degradation; this appears to indicate that the cleanliness and seal integrity of the system may permit several years of operation. We are presently installing a new amplifier, PHA and timer control, that will significantly reduce the size and mass of the second container. It will also reduce power consumption of the system to about 1W, permitting battery operation over several days.

The predicted intrinsic resolution of xenon at 662 keV is just under 0.6% FWHM. The best resolution measured in this work is 2% (figure 7). The excellent results reported in ref. [15] provide encouraging experimental evidence that the intrinsic gas resolution is, indeed, close to the prediction, at least for densities below 0.6 g/cm^3. Our future plans include studies to reduce further the measured resolution in a practical device; we will also investigate the option of using cylindrical counter geometry [5], which allows more efficient use of xenon in a given volume.

VII. Acknowledgments

The motivation for this work came from Dr. John Markey, whose input in the initial design phase was most helpful. We also appreciate insightful discussions with Dr. Aleksey Bolotnikov.

VIII. References

[1] U. Fano, "Ionization Yield of Radiations. II. The Fluctuations of the Number of Ions," *Phys. Rev.* 72 (1947) 26-29.

[2] H. Sipilä, "The Statistics of Gas Gain in Penning Mixtures," *IEEE Trans. Nucl. Sci.* NS-26 (1979) 181-185.

[3] C.R. Gruhn and R. Loveman, "A Review of the Physical Properties of Liquid Ionization Chamber Media," *IEEE Trans. Nucl. Sci.* NS-26 (1979) 110-119.

[4] V.A. Rabinovitch, A.A. Vasserman, V.I. Nedostup and L.S. Veksler, Thermophysical Properties of Neon, Argon, Krypton and Xenon, Hemisphere Publ. Co., 1985.

[5] A. Bolotnikov and B.D. Ramsey, "Improving the Energy Resolution of High-pressure Xe Cylindrical Ionization Chambers," *IEEE Trans. Nucl. Sci.* NS-44 (1997) 1006-1010.

[6] V.V. Dmitrenko, A.S. Romanyuk, S.I. Suchkov and Z.M. Uteshev, "Compressed-Xenon Ionization Chamber for Gamma Spectroscopy," *Sov. Phys. –Tech. Phys. (USA)* 28 (1983) 1440.

[7] C. Levin, J. Germani and J. Markey, "Charge collection and energy resolution studies in compressed xenon gas near its critical point," *Nucl. Instrum. & Meth. In Phys. Res.* A332 (1993) 206-214.

[8] G. Tepper and J. Losee, "High resolution room temperature ionization chamber xenon gamma radiation detector," *Nucl. Instrum. & Meth. In Phys. Res.* A356 (1995) 339-346.

[9] O. Bunemann, T.E. Cranshaw and J.A. Harvey, "Design of Grid Ionization Chambers," *Can. J. of Res.* A27 (1948) 191-206.

[10] Ceramaseal, P.O. Box 260/U.S. Route 20, New Lebanon, NY 12125.

[11] Span Instruments, P.O. Box 860709, Plano, TX 75086-0709.

[12] UltraPure System Inc., PO Box 60160, Colorado Springs, CO 80960.

[13] Advanced Products Co., 33 Defco Park Rd., North Haven, CT 06473.

[14] A. Bolotnikov and B.D. Ramsey, "Purification Techniques and Purity and Density Measurements of High-pressure Xe," *Nucl. Instrum. & Meth. In Phys. Res.* A383 (1996) 619-623.

[15] A. Bolotnikov and B.D. Ramsey, "The Spectroscopic Properties of High Pressure Xenon," *Nucl. Instrum. & Meth. In Phys. Res.* A396 (1997) 360-370.